

Comparison of models and measurements of protons of trapped and secondary origin with PAMELA experiment.

N. De Simone^{xvii}, O. Adriani^{†*}, G. C. Barbarino^{‡§}, G. A. Bazilevskaya[¶], R. Bellotti^{||**},
M. Boezio^{††}, E. A. Bogomolov^{‡‡}, L. Bonechi^{†*}, M. Bongi^{*}, V. Bonvicini^{††}
S. Bottai^{*}, A. Bruno^{||**}, F. Cafagna^{||}, D. Campana[§], P. Carlson^{xviii}, M. Casolino^x, G. Castellini^{xiv}
C. De Santis^{xvii}, M. P. De Pascale^{xvii}, G. De Rosa[§], V. Di Felice^{xvii}, A. M. Galper[¶]
L. Grishantseva^{xi}, P. Hofverberg^{xiii}, S. V. Koldashov^{xi}, S. Y. Krutkov^{‡‡}, A. N. Kvashnin[¶], A. Leonov^{xi}
L. Marcelli^x, W. Menn^{xv}, V. V. Mikhailov^{xi}, E. Mocchiutti^{††}, N. Nikonov^{‡‡}, G. Osteria[§], P. Papini^{*},
M. Peroni^{xii}, M. Pearce^{xiii}, P. Picozza^{xvii}, M. Ricci^{xvi}, S. B. Ricciarini^{*}, M. Simon^{xv}, R. Sparvoli^{xvii},
P. Spillantini^{†*}, Y. I. Stozhkov[¶], A. Vacchi^{††}, E. Vannuccini^{*}, G. Vasilyev^{‡‡}, S. A. Voronov^{xi},
Y. T. Yurkin^{xi}, G. Zampa^{††}, N. Zampa^{††}, and V. G. Zverev^{xi}

* INFN, Sezione di Firenze Via Sansone 1, I-50019 Sesto Fiorentino, Florence, Italy

† University of Florence, Department of Physics, Via Sansone 1, I-50019 Sesto Fiorentino, Florence, Italy

‡ University of Naples "Federico II", Department of Physics, Via Cintia, I-80126 Naples, Italy

§ INFN, Sezione di Naples, Via Cintia, I-80126 Naples, Italy

¶ Lebedev Physical Institute, Leninsky Prospekt 53, RU-119991 Moscow, Russia

|| University of Bari, Department of Physics, Via Amendola 173, I-70126 Bari, Italy

** INFN, Sezione di Bari, Via Amendola 173, I-70126 Bari, Italy

†† INFN, Sezione di Trieste, Padriciano 99, I-34012 Trieste, Italy

‡‡ Ioffe Physical Technical Institute, Polytekhnicheskaya 26, RU-194021 St. Petersburg, Russia

^x INFN, Sezione di Roma "Tor Vergata", Via della Ricerca Scientifica 1, I-00133 Rome, Italy

^{xi} Moscow Engineering and Physics Institute, Kashirskoe Shosse 31, RU-11540 Moscow, Russia

^{xiii} University of Rome "Tor Vergata", Department of Physics, Via della Ricerca Scientifica 1, I-00133 Rome, Italy

^{xviii} KTH, Department of Physics, AlbaNova University Centre, SE-10691 Stockholm, Sweden

^{xiv} IFAC, Via Madonna del Piano 10, I-50019 Sesto Fiorentino, Florence, Italy

^{xv} Universität Siegen, D-57068 Siegen, Germany

^{xvi} INFN, Laboratori Nazionali di Frascati, Via Enrico Fermi 40, I-00044 Frascati, Italy

Abstract. PAMELA is a satellite borne experiment designed to study with great accuracy cosmic rays of galactic, solar, and trapped nature in a wide energy range (protons: 80 MeV-700 GeV, electrons 50 MeV-400 GeV). Main objective is the study of the antimatter component: antiprotons (80 MeV-190 GeV), positrons (50 MeV-270 GeV) and search for antinuclei with a precision of the order of 10^{-8} . The experiment, housed on board the Russian Resurs-DK1 satellite, was launched on June, 15th 2006 in a 350×600 km orbit with an inclination of 70 degrees. In this work we present the measurement of galactic and reentrant albedo proton spectra in the energy range between 100 MeV and 300 GeV. The galactic protons refer to the period 2006-2008, showing evidence of Solar modulation effects even during the solar minimum.

Keywords: cosmic rays, antimatter, dark matter, solar particle events, trapped cosmic rays

I. MEASUREMENT OF COSMIC RAYS IN EARTH'S MAGNETOSPHERE

Earth's magnetic field can be used as a spectrometer to separate cosmic rays of various nature and origin. To separate the primary (galactic) component from the reentrant albedo (particles produced in interactions of cosmic rays with the atmosphere below the cutoff and propagating along Earth's magnetic field line) component it is necessary to evaluate the local geomagnetic cutoff. This is estimated using the IGRF magnetic field model along the orbit; from this the McIlwain L shell is calculated[1]. In this work we have used the vertical Stormer (defined as $G = 14.9/L^2$) approximation[2] to separate between particles of different nature. Figure 2 shows the rigidity of particles as function of the evaluated cutoff G . The primary (galactic) component, with rigidities above the cutoff is clearly separated from the reentrant albedo (below cutoff) component, containing also trapped protons in the South Atlantic Anomaly (SAA).

Cuts in the energy loss (dE/dx) vs rigidity remove positrons, pions and $Z \geq 2$ as shown in figure 1.

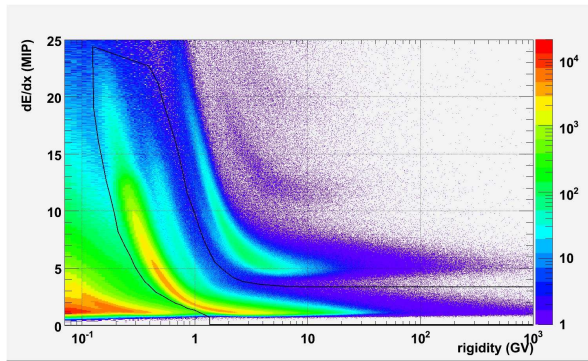


Fig. 1: Energy loss in tracker (mean in all planes hit) vs tracker rigidity for positively charged particles. The Proton and Helium bands are clearly visible. The black lines represent cuts used to select protons.

Since energy loss of a charged particle follows Bethe Block formula, $dE/dx \propto Z^2/\beta^2$ (neglecting logarithmic terms), the measurement of the average energy released in the tracker planes for a given event at a given rigidity can be used to discriminate between different particles. The topmost band in the Figure is due to helium nuclei which have energy loss in the tracker $Z^2 = 4$ times the protons, identified in the central band. Bottom left releases are due to positrons, relativistic also at low rigidities and the background of pion and secondary particles. The black line shows the energy dependent cuts used to select a proton sample. From the Figure it is also possible to identify at low rigidities the deuterium contribution, resulting in a band with higher energy releases due to the lower β for a given rigidity due to the double atomic number A of deuterium. In this analysis deuterium and protons have been considered together with the term proton implying $Z = 1$, $A = 1, 2, 3$.

A. Trapped particles in the Van Allen Belts

The high energy ($> 80\text{MeV}$) component of the proton belt, crossed in the South Pacific region can be monitored in detail with PAMELA. In figure II is shown the differential energy spectrum measured in different regions of the South Atlantic Anomaly. Proton selection criteria are the same used in the determination of the absolute galactic spectrum. It is possible to see the increase of the flux toward the centre of the anomaly. Particle flux exceeds several orders of magnitude the flux of secondary (reentrant albedo) particles measured in the same cutoff region outside the anomaly and it is maximum where the magnetic field is lowest. The trapped component at the center can be fitted with energy dependent power law spectrum of the form $\phi = AE^{-\gamma-\delta E}$. This measurement can be used to validate various existing models[3], [4] providing information on the trapping and interaction processes in Earth's magnetosphere. These studies will be expanded to address temporal and spatial variations as well as

Region G	A $p/cm^2 s sr GeV$	γ	δ GV^{-1}	χ^2 $/ndf$
$0.19 < B$	4.0 ± 0.4	3.6 ± 0.6	2.0 ± 0.4	0.04
$0.19 < B < 0.20$	1.0 ± 0.1	4.6 ± 0.8	1.6 ± 0.5	0.17
$0.20 < B < 0.21$	0.05 ± 0.008	5.6 ± 1.5	0.8 ± 1.4	0.40

TABLE I: Fit of the core regions of the SAA according to a rigidity dependent power law spectrum.

different particle species such as antiprotons[5]. These results can be scaled to larger but less directly accessible - magnetospheres such as Jupiter or pulsars. In Table I are shown the values obtained fitting the trapped spectra with a rigidity dependent power law $\phi_{tr} = AR^{-\gamma-\delta R}$. In figure 4 is shown the comparison between the fluxes measured with PAMELA at the center of the SAA and the model described in [4]. In order to have a detailed comparison we have restricted to a small range in latitude, longitude and altitude. It is possible to see that there is a good agreement, especially below 600 MeV between model and experimental data. At higher energies the model gives a lower flux, possibly due to the finite aperture of PAMELA or a limit in the trapping mechanism. Future work will involve the comparison of this model also for antiprotons.

B. Secondary particles production in the Earth's atmosphere

In figure 3 is shown the particle flux measured in different cutoff regions. It is possible to see the primary (galactic - above cutoff) and the secondary (reentrant albedo - below cutoff) component. At the poles, where field lines are open and cutoff is below the minimum detection threshold of PAMELA the secondary component is not present. Moving toward lower latitude regions the cutoff increases and it is possible to see the two components, with the position of the gap increasing with the increase of the cutoff. The secondary component of cosmic rays contributes to the atmospheric neutrino production[6]. Therefore an accurate measurement of the secondary component is of relevance in the reduction of the uncertainties of the expected flux on the ground[7] and in the estimation of hadronic cross sections (protons on O or N) at high energies, not otherwise determinable on ground.

REFERENCES

- [1] Tech. rep., IAGA (2005).
- [2] M. A. Shea, et al., Physics of the Earth and Planetary Interiors 48 (1987) 200–205.
- [3] J. D. Gaffey, Jr., et al., Journal of Spacecraft and Rockets 31 (1994) 172–176.
- [4] R. S. Selesnick, et al., Space Weather 5 (2007) S04003.
- [5] R. S. Selesnick, et al., Geophysical Research Letters 34 (2007) 20104+.
- [6] M. Honda, et al., Physical Review D70 (4) (2004) 043008+.
- [7] T. Sanuki, et al., Physical Review D75 (4) (2007) 043005+.

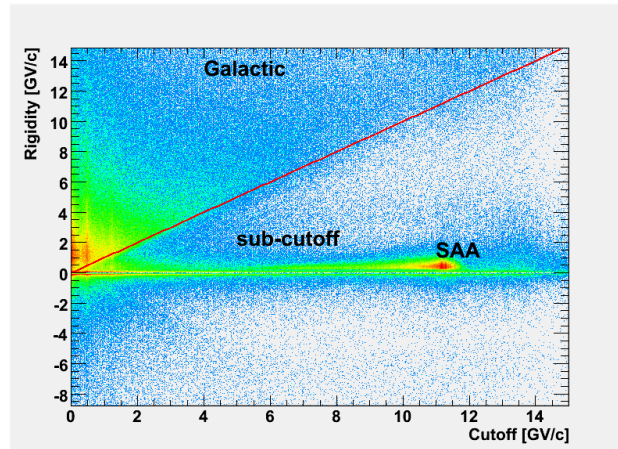


Fig. 2: Histogram of the rigidity R_{tr} measured in the tracker vs vertical Stormer Cutoff. Particles with positive charge (p, e^+) have $R_{tr} > 0$ and particles with negative charge have $R_{tr} < 0$. The effect of the geomagnetic field on galactic particles is clearly visible. Primary particles, of galactic or solar origin, have a rigidity above the local Stormer cutoff (see text) and are well separated from reentrant albedo events (below the cutoff) produced in the interaction of primaries with the Earth’s atmosphere. It is also possible to see the spot of high fluence of low ($R < 2$ GV) protons trapped in the inner Van Allen belt, crossed by PAMELA in the South Atlantic Anomaly (SAA) region.

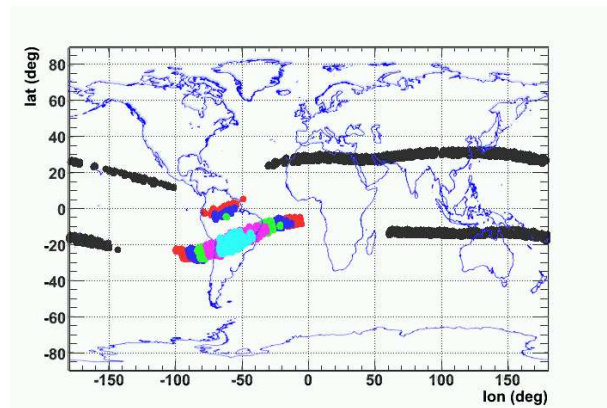
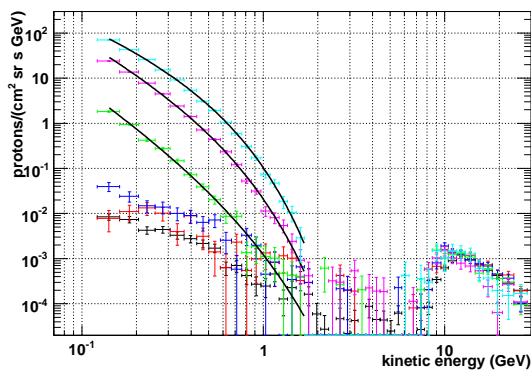


TABLE II: Left: Plot of the differential energy spectrum of PAMELA in different regions of the South Atlantic Anomaly. Selection regions (shown in right panel) are selected according to decreasing intensity of the magnetic field from bottom to top: Black $B > 0.3$ G - outside the SAA, Red 0.22 G $< B < 0.23$ G, Blue 0.21 G $< B < 0.22$ G, Green 0.20 G $< B < 0.21$ G, Pink 0.19 G $< B < 0.20$ G, Turquoise 0.19 G $> B$) in the cutoff region 10.8 GV $< G < 11.5$ GV. Flux of trapped particles can exceed the secondary particle flux in the same cutoff region outside the anomaly (black bands) of about four orders of magnitude at low energy.

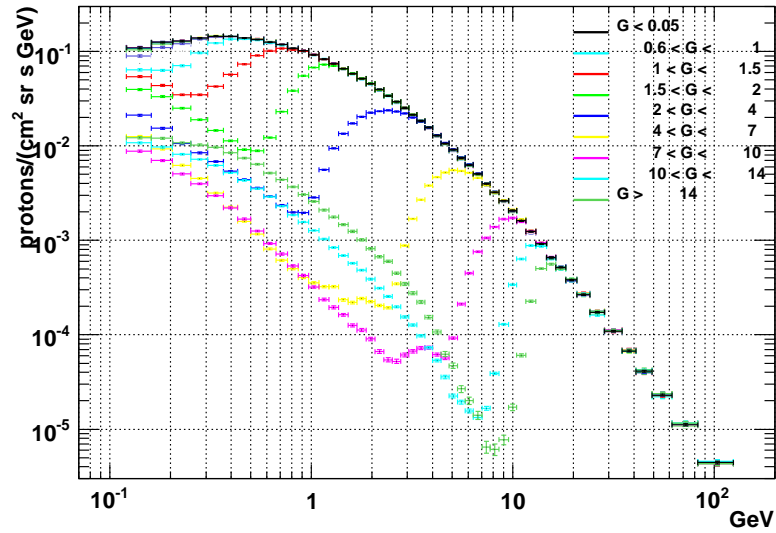


Fig. 3: Plot of the differential energy spectrum of PAMELA at different values of geomagnetic cutoff G . It is possible to see the primary spectrum at high rigidities and the reentrant albedo (secondary) flux at low rigidities. Only statistical errors are shown.

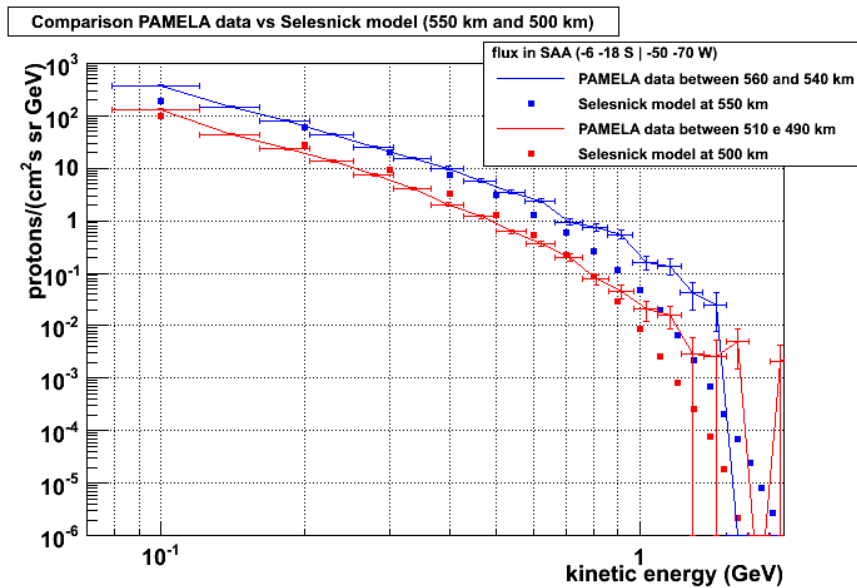


Fig. 4: Comparison of the differential spectrum measured with PAMELA and evaluated using the method described in [4].